Dalton Transactions

ROYAL SOCIETY OF CHEMISTRY

PAPER

View Article Online
View Journal | View Issue

Cite this: *Dalton Trans.*, 2022, **51**, 14491

The effect of the hydroxyl group position on the electrochemical reactivity and product selectivity of butanediol electro-oxidation†

Shengnan Sun,‡[a,b] Chencheng Dai,‡[a] Libo Sun,[a] Zhi Wei Seh,[b] Yuanmiao Sun,[a] Adrian Fisher,[c] Xin Wang[d,e] and Zhichuan J. Xu*[a,e,f]

Received 28th July 2022,
Accepted 21st August 2022

DOI: 10.1039/d2dt02450k

rsc.li/dalton

This article presents a study on the effect of the hydroxyl group position on the electro-oxidation of butanediols, including 1,2-butanediol, 2,3-butanediol, 1,3-butanediol, and 1,4-butanediol. The effect of the hydroxyl group position in butanediols on their electro-oxidation reactivities is investigated by cyclic voltammetry, linear sweep voltammetry, chronopotentiometry and chronoamperometry in 1.0 M KOH. The results show that the closer the two hydroxyl groups are, the higher the reactivity, and the lower the anodic potential butanediol has. Moreover, the oxidation products from chronoamperometry are analyzed by means of HPLC and NMR. Some value-added products, such as 3-hydroxypropionic acid/3-hydroxypropionate, are produced. The DFT calculation indicates that the oxidation of vicinal diols responds to the conversion from a hydroxyl group to a carboxylate group, followed by C–C bond cleavage, where the carbon charge decreases. These results provide an insight into reactant selection for the electrochemical synthesis of value-added chemicals.

1. Introduction

In recent decades, the electro-oxidation of small molecule alcohols has been studied extensively due to the interest in their potential as raw materials for the electro-synthesis of value-added chemicals and alternative reactions of the oxygen evolution reaction (OER) for H_2 cogeneration.[1–5] The electro-oxidation of alcohols has been investigated on both noble metal[6–8] and non-noble metal-based electrodes,[9,10] and also their hybrid electrodes.[11–13] A number of studies have been focused on improving the catalytic activity of electrodes as well as reducing the mass loading of noble metals.[14,15] On the other hand, due to their abundant reserve and low cost, first row transition metal oxides, such as cobalt and nickel based oxides, have become increasingly attractive with regard to the oxidation of these small alcohols.[16–20] For example, Co_3O_4, as one of the most investigated electrode materials, consisting of one Co^{2+} at the tetrahedral site and two Co^{3+} ions at the octahedral site within a cubic spinel structure, has been extensively studied for alcohol electro-oxidation[16,17] and meanwhile effort has also been devoted to optimizing the electro-oxidation activities of Co_3O_4 with other transition metal substitutions and modifications.[18–20]

Despite much effort being devoted to the modification of cobalt-based oxides to achieve higher activity for alcohol oxidation, rare attention has been paid to the alcohol itself. Electro-oxidation of alcohols often proceeds *via* the processes of hydroxyl group conversion and C–C bond scission. The position and number of hydroxyl groups in alcohol molecules affect the alcohol reactivity. On both Au and Pt electrodes, polyhydric alcohols are found to be more reactive than the monohydric ones.[21,22] Further study on the influence of the hydroxyl group position on diol electro-oxidation has been conducted on noble metals.[21–25] For example, 2,3-butanediol (2,3-BD) exhibits higher reactivity than 1,3-butanediol (1,3-BD) and 1,4-butanediol (1,4-BD) on Au, which is explained by the strong resonance effect of hydroxyl groups in 2,3-BD.[26] In spite of numerous and relevant investigations, to our knowledge, limited attention has been paid to non-noble metal oxides.

[a]*School of Material Science and Engineering, Nanyang Technological University, 50 Nanyang Avenue, 639798 Singapore. E-mail: xuzc@ntu.edu.sg*
[b]*Institute of Materials Research and Engineering, Agency for Science, Technology and Research (A*STAR), 2 Fusionopolis Way, 138634 Singapore*
[c]*Department of Chemical Engineering and Biotechnology, University of Cambridge, West Cambridge Site, Philippa Fawcett Drive, CB3 0AS Cambridge, UK*
[d]*School of Chemical and Biomedical Engineering, Nanyang Technological University, 62 Nanyang Drive, Singapore 637459, Singapore*
[e]*Centre of Advanced Catalysis Science and Technology, Nanyang Technological University, 50 Nanyang Avenue, 639798 Singapore*
[f]*Energy Research Institute @ Nanyang Technological University, ERI@N, Interdisciplinary Graduate School, Nanyang Technological University, 50 Nanyang Avenue, 639798 Singapore*

†Electronic supplementary information (ESI) available. See DOI: **https://doi.org/10.1039/d2dt02450k**

‡These authors contributed equally.

Subsequently, the influence of the hydroxyl position on the diol compound electro-oxidation on non-noble oxides is poorly understood, and therefore it is of interest to investigate the diol compound electro-oxidation behavior on non-noble metal oxides from both experimental and computational aspects. Due to multiple possible oxidation reactions on the diol compounds, investigating and taking advantage of the priority and mechanism behind hydroxyl group conversion and C–C bond selective scission for electro-synthesizing target value-added products are significant.

Compared to our previous work on C3 alcohol oxidation,[15] aliphatic butanediols have three C–C bonds and more possibilities of being converted into C1, C2, C3, and C4 compounds during the C–C selective cleavage. Meanwhile, due to the presence of two hydroxyl groups, the oxidation product diversity is increased. Herein, this work systematically investigates the influence of the hydroxyl group position on the electro-oxidation behavior of a series of butanediols, including 1,2-butanediol (1,2-BD), 1,3-butanediol, 1,4-butanediol, and 2,3-butanediol on the Co_3O_4 electrode in alkaline media. First, the diol electro-oxidation behavior is studied by means of cyclic voltammetry (CV) and chronopotentiometry (CP) approaches. Then the diol concentration effect is also investigated by the CP approach. The oxidation products are analyzed by high-performance liquid chromatography (HPLC) and nuclear magnetic resonance (NMR) approaches. Finally, density functional theory (DFT) calculations are employed to analyze the hydroxyl group position effect by comparing the energy barriers of reaction pathways and carbon density changes during oxidation.

2. Results and discussion

First, the electro-oxidation properties of butanediols are investigated by means of cyclic voltammetry due to their complicated structures. From the first 100 continuous CV curves of Co_3O_4 in 1.0 M KOH in the absence and presence of diols (Fig. S1†), the prominent oxidation current drop for all these diols suggests that the oxidation intermediate products gradually adsorb and accumulate on the electrode surface. These intermediate products normally form during the dissociative chemisorption of alcohol, and act as catalyst poisons that diminish the electrode activity considerably.[27] The CV cycle of diol oxidation (Fig. 1a) indicates that the diol reactivities are in the order of 1,2-BD > 2,3-BD > 1,3-BD > 1,4-BD, as discerned from the potential at 5 mA (Fig. S2a†) and the oxidation current (Fig. S2b†). Among these, 1,2-BD is oxidized at the lowest potential (*ca.* 1.354 V), while 1,4-BD is the most difficult to oxidize (*ca.* 1.412 V). In terms of the oxidation potential from a dynamic CV test, these four diols have two oxidation potential regions. Oxidation of 1,2-BD and 2,3-BD starts in the relatively low potential region, while 1,3-BD and 1,4-BD start to be oxidized in the relatively high potential region. Considering their molecular structures, both 1,2-BD and 2,3-BD bear vicinal hydroxyl groups, while the other diols do not. It appears that the oxidation of diols with vicinal hydroxyl

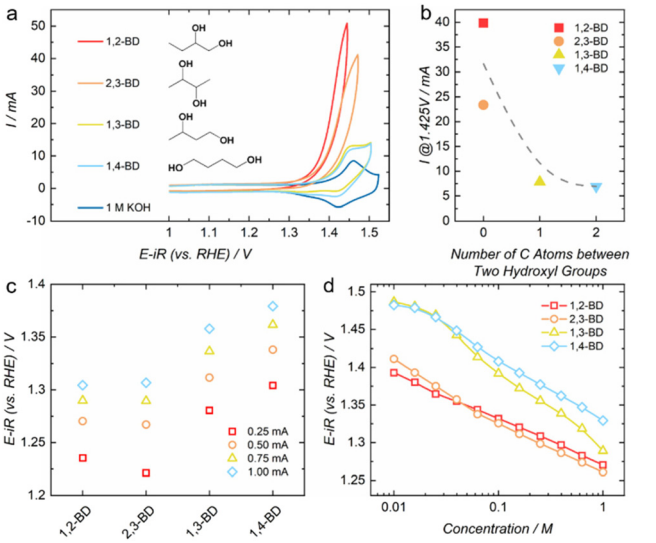

Fig. 1 (a) The CV curves of butanediol oxidation in 1.0 M KOH at 10 mV s^{-1}; (b) the dependence of the anodic current of diols at 1.425 V *vs.* RHE on the number of C atoms between two hydroxyl groups; (c) the CP limiting potentials of butanediol oxidation at different applied currents; (d) concentration dependence of the potential for diol oxidation in CP tests.

groups takes place at relatively low potentials, compared to the oxidation of diols without vicinal hydroxyl groups. These results indicate that alcohol reactivity can be influenced by the position of hydroxyl groups. Vicinal diols are more reactive than others. Besides, as shown in Fig. 1b, the closer these two hydroxyl groups are, the easier the alcohols are oxidized. When the vicinal hydroxyl groups are located at the terminal position, the corresponding alcohols are more easily oxidized. To minimize the influence of the current from double-layer capacitance, pseudo-capacitance, the oxygen evolution reaction at a high potential, and the dynamic influence in CV tests, steady-state CP curves are used to investigate the butanediol oxidation potential at 0.25, 0.50, 0.75, and 1.00 mA (Fig. 1c and S3†). It is observed that the potential at 0.25 mA is in the order 1,2-BD, 2,3-BD (1.22–1.23 V) < 1,3-BD (1.27–1.28 V) < 1,4-BD (1.30 V). Similar potential orders are also found at 0.50, 0.75 and 1.00 mA. For example, at 1.00 mA, 1,2-BD, 2,3-BD (1.30–1.31 V) < 1,3-BD, 1,4-BD (1.36–1.38 V). The CP results indicate that 1,2-BD and 2,3-BD are the easiest to be oxidized, which bear the vicinal hydroxyl groups. In contrast, 1,3-BD and 1,4-BD, without vicinal hydroxyl groups, have relatively high oxidation potentials. Among these, 1,4-BD with the longest distance between hydroxyl groups is the diol most difficult to oxidize. Besides, compared with the OER potential, the addition of 1,2-BD and 2,3-BD leads to a potential drop of more than 0.2 V, and even the addition of the least active butanediol, 1,4-BD, can reduce the potential by approximately 0.15 V. These results suggest that the butanediol oxidation reaction is thermodynamically more favorable than the OER on the Co_3O_4 electrode in an alkaline electrolyte. To investigate the diol concentration effect, CP curves at 0.5 mA (Fig. 1d and S4†) are recorded at diol concentrations from 0.01 to 1.00

M. Obviously, the resultant potential becomes lower and lower with the increasing diol concentration. Meanwhile no potential saturation is observed in this concentration range. However, a dramatic potential drop is noticed when the diol concentration increases from 0 to 0.01 M for the diols with vicinal hydroxyl groups (1,2-BD and 2,3-BD in Fig. S4a and b†). In contrast, for the diols lacking vicinal hydroxyl groups (1,3-BD and 1,4-BD in Fig. S4c and d†), the potential is still close to the OER potential. The resultant potential summary (Fig. 1d) shows two distinct regions from 0.01 to 1.00 M. Those diols bearing vicinal hydroxyl groups (1,2-BD and 2,3-BD) have obviously lower potentials compared to those diols without vicinal hydroxyl groups. The potential difference between these two types of diols is more obvious at lower concentrations. The value of the potential can be obtained from the slope of E *vs.* $\log C$ according to the following equation:

$$i = nFAk_0C \times \exp(n\beta F(E - E^{\theta\prime})/RT),$$

$$E = (-2.303RT/\beta nF) \times \log(nFAk_0C) + (2.303RT/\beta nF) \times \log i + E^{\theta\prime},$$

where i is the applied current; n is the number of electrons involved in the rate-determining step; F, A, k_0, C, R, and T are the faradaic constant, electrode area, kinetic coefficient, diol concentration, gas constant, and temperature, respectively; $E^{\theta\prime}$ and E are the formal potential and the resultant potential, respectively; and β is the electron transfer coefficient.[28] To lower the effect of diffusion limitation, the fitted concentration region is chosen at a relatively high concentration from 0.10 to 1.00 M to increase the concentration gradient. The values of βn at 0.5 mA are 0.95, 0.92, 0.60, and 0.76 for 1,2-BD, 2,3-BD, 1,3-BD and 1,4-BD, respectively. The difference suggests that the βn values of 1,2-BD and 2,3-BD with vicinal hydroxyl groups are larger than those of the others.

The HPLC and NMR analyses of the electrolyte solutions after the butanediol oxidation at 1.524 V *vs.* RHE in 1 M KOH (Fig. S6†) can be found in Fig. 2a and Fig. S7 and S8,† respectively. The NMR peak attribution is based on the NMR spectra of these butanediols in KOH and our previous report.[14] As shown in Fig. 2a and b, it can be concluded that the major products of 1,2-BD and 2,3-BD oxidation are formate and propionate, and acetate, respectively. All these products are produced after C–C bond cleavage. In contrast, the molar percentages of products without C–C bond cleavage for 1,3-BD (3-hydroxybutyrate) and 1,4-BD (4-hydroxybutyrate and succinate) are significantly larger. This observation suggests that the C–C bonds bearing vicinal hydroxyl groups are more easily broken down. It is worth mentioning that some reaction pathways (Scheme 1) can potentially be employed for the preparation of value-added products with decent selectivity (shown in Table 1). For example, 3-hydroxypropionic acid is a potential platform chemical for acrylic acid synthesis.[29] Acetic acid can be produced from 2,3-butanediol with 100 mol% selectivity. Acetic acid has a wide range of applications, including production of chemicals, purification of organics, medical uses,

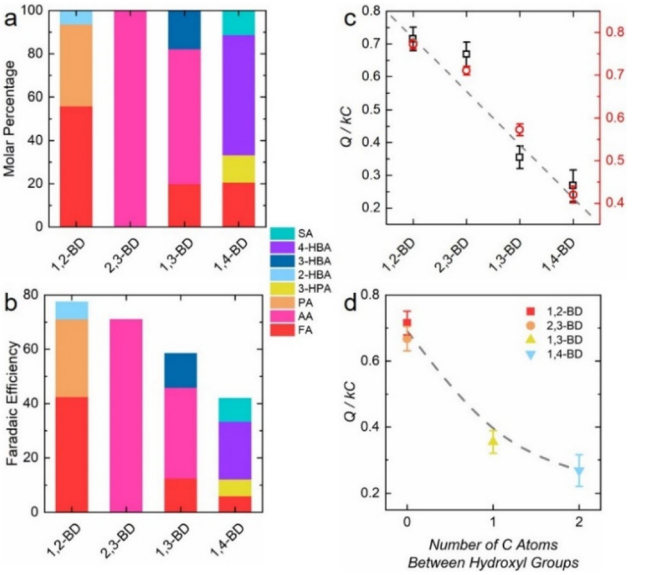

Fig. 2 Product distribution of 0.75 M 1,2-butanediol (1,2-BD), 2,3-butanediol (2,3-BD), 1,3-butanediol (1,3-BD), and 1,4-butanediol (1,4-BD) electro-oxidation at 1.524 V *vs.* RHE in 1 M KOH electrolyte based on (a) molar percentage and (b) faradaic efficiency. (c) Total charge transferred and the sum of faradaic efficiencies of all products during the CA measurement for electro-oxidation of the above-mentioned diols. (d) The dependence of total charge transferred on the number of C atoms between hydroxyl groups. AA: acetate; FA: formate; 3-HPA: 3-hydroxypropionate; PA: propionate; 2-HBA: 2-hydroxybutyrate; 3-HBA: 3-hydroxybutyrate; 4-HBA: 4-hydroxybutyrate; SA: succinate.

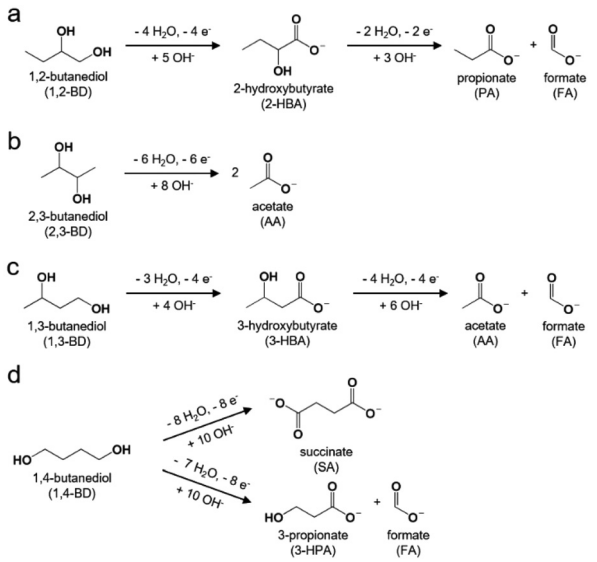

Scheme 1 Proposed reaction pathways of (1) 1,2-butanediol (1,2-BD), (2) 2,3-butanediol (2,3-BD), (3) 1,3-butanediol (1,3-BD), and (4) 1,4-butanediol (1,4-BD) electro-oxidation in 1 M KOH on the basis of product analysis from NMR and HPLC.

and as a food additive. In addition, as shown in Fig. 2c, the total charge transferred during the CA measurements of diol electro-oxidation represents the order of reactivities of butane-

Table 1 Product selectivities from diol electro-oxidation and their main applications

Product	Substrate	Selectivity (molar%)	Main applications
Formic acid (formate)	1,2-Butanediol	81.9%	Cleaning, biocides, leather processing, textile processing, food preservation, latex coagulation, flue gas desulfurization, drilling fluids, and de-icing
	1,3-Butanediol	19.7%	
	1,4-Butanediol	20.4%	
Acetic acid (acetate)	2,3-Butanediol	100%	Production of chemical compounds, purification of organic compounds, medical use, and food additives
3-Hydroxypropionic acid (3-hydroxypropionate)	1,4-Butanediol	12.7%	Production of chemical compounds and biodegradable polymer precursors
2-Hydroxybutyric acid (2-hydroxybutyrate)	1,2-Butanediol	6.5%	Biomarkers
3-Hydroxybutyric acid (3-hydroxybutyrate)	1,3-Butanediol	18%	Biodegradable polymer precursors
Succinic acid (succinate)	1,4-Butanediol	11.5%	Precursors to polymers, resins and solvents, and food and dietary supplements

diols as 1,2-BD > 2,3-BD > 1,3-BD > 1,4-BD, which is consistent with the results mentioned above. Moreover, Fig. 2d demonstrates that the closer the two hydroxyl groups are, the higher the amount of charge transferred. This observation is consistent with the study of diol reactivity by CV (shown in Fig. 1b). The total faradaic efficiency (FE) of all products is also investigated (Fig. 2b). Since the CA measurements were conducted near the OER region, the reactivity of the diol is crucial for the competition between the OER and diol oxidation. The higher butanediol reactivity leads to a more dominant butanediol electro-oxidation rate in the competition, and hence results in a higher total FE towards organic salt production during the CA test. Consequently, the order of total FE from diol oxidation is in agreement with the order of the diol reactivities.

A similar hydroxyl group position effect has also been observed on noble metals, such as –Au and Pt, where the electroactivity is higher for the isomers of diols carrying hydroxyl groups at vicinal positions than it is for terminal isomers.[21,23,25–27,30,31] The higher reactivity for diols with vicinal hydroxyl groups is a result of a lower dehydrogenation barrier than that found for diols with terminal hydroxyl groups. In alkaline media, deprotonation takes place as follows: (1) the first step is the base-catalyzed deprotonation of H_α from an alcohol ($H_\beta R–OH_\alpha$) into a reactive alkoxide intermediate; and (2) the second step is the deprotonation of H_β from an alkoxide catalyzed by an electrode material.[6,32] When the electrolyte pH and electrode material are fixed, the possible explanation for the easier dehydrogenation of diols with vicinal hydroxyl groups is the lower energy of the C–H_β bond in $H_\beta R–OH_\alpha$ for vicinal isomers, relative to the energy of the C–H_β bond in terminal isomers.

Subsequently, the hydroxyl group position effect is further investigated by DFT calculations. The adsorption of butanediols and oxidation intermediates on the Co_3O_4-(111) surface, and the calculated electronic energies of the corresponding dehydrogenation and oxidation steps are shown in Fig. 3 and Fig. S9.† All the reaction pathways can be found in Tables S1–S4.† In order to describe the carbon atoms in these butanediols clearly, we labelled them C1, C2, C3 and C4, respectively, as shown in Fig. 3 and Fig. S9.† The primary butanediols 1,2-BD, 1,3-BD and 1,4-BD and the secondary butanediol 2,3-BD have different dehydrogenation and oxidation reaction pathways. The primary butanediol RCH_2OH (R = CH_3CH_2CHOH, $CH_3CHOHCH_2$ or $CH_2OHCH_2CH_2$) is first adsorbed and dehydrogenated to form RCH_2O^*. The obtained RCH_2O^* then, through two oxidative dehydrogenation steps, forms RCO*, which is further oxidized to form the first carboxylic group. In this process, the oxidative dehydrogenation occurs on the carbon atom with the hydroxyl group, where the oxygen atom is adsorbed. After the formation of the first carboxylic group, the dehydrogenation and oxidation proceed on the other carbon atoms. The following dehydrogenation and oxidation pathways on 1,2-BD, 1,3-BD, and 1,4-BD are different. For 1,2-BD with a vicinal hydroxyl group (Fig. 3a and e), further dehydrogenation and oxidation occur on the carbon atom C2 with a hydroxyl group until $–C(OH)_2–$ forms, followed by the cleavage of the C–C bond. Analysis of the 1,2-BD oxidation intermediate species indicates that the relative energy change from the initial state to the first –CO state reaches 2.491 eV, and then decreases to −1.086 eV when –COO– forms. The relative energy increases again for the dehydrogenation of the carbon atom C2; however, the energy is as low as 0.118 eV. From the aspect of carbon charge, the decrease degrees of C1 and C2 are different. The calculated C1 charge decreases from 3.719 to 2.509, from $–CH_2O$ to –COOH. The calculated charge of the C2 carbon atom with the hydroxyl group starts to decrease dramatically from –CHOH– (3.506), –COH– (3.482) to $–C(OH)_2–$ (3.010). After that, the C–C bond cleavage happens. After cleavage, the charge of this carbon atom further decreases to 2.578. The charges of C3 and C4 atoms, which are not involved in the bond cleavage, remain high (at around 4) and do not show any obvious change. Overall, for 1,2-BD, the C–C bond cleavage is a process in which the charge of both neighboring carbon atoms decreases. When both are lower than 3, the C–C bond cleavage happens. Compared to 1,2-BD, 1,3-BD has a more complicated process because the carbon atoms with hydroxyl groups are not vicinal (Fig. 3c and g). The calculation analysis shows that adsorption happens on the oxygen linked with the C1 atom, and $–CH_2OH$ gradually becomes a carboxylic group along with the relative energy increasing and then decreasing, as well as a decrease in the charge of carbon atoms. Differing from 1,2-BD, further dehydrogenation and

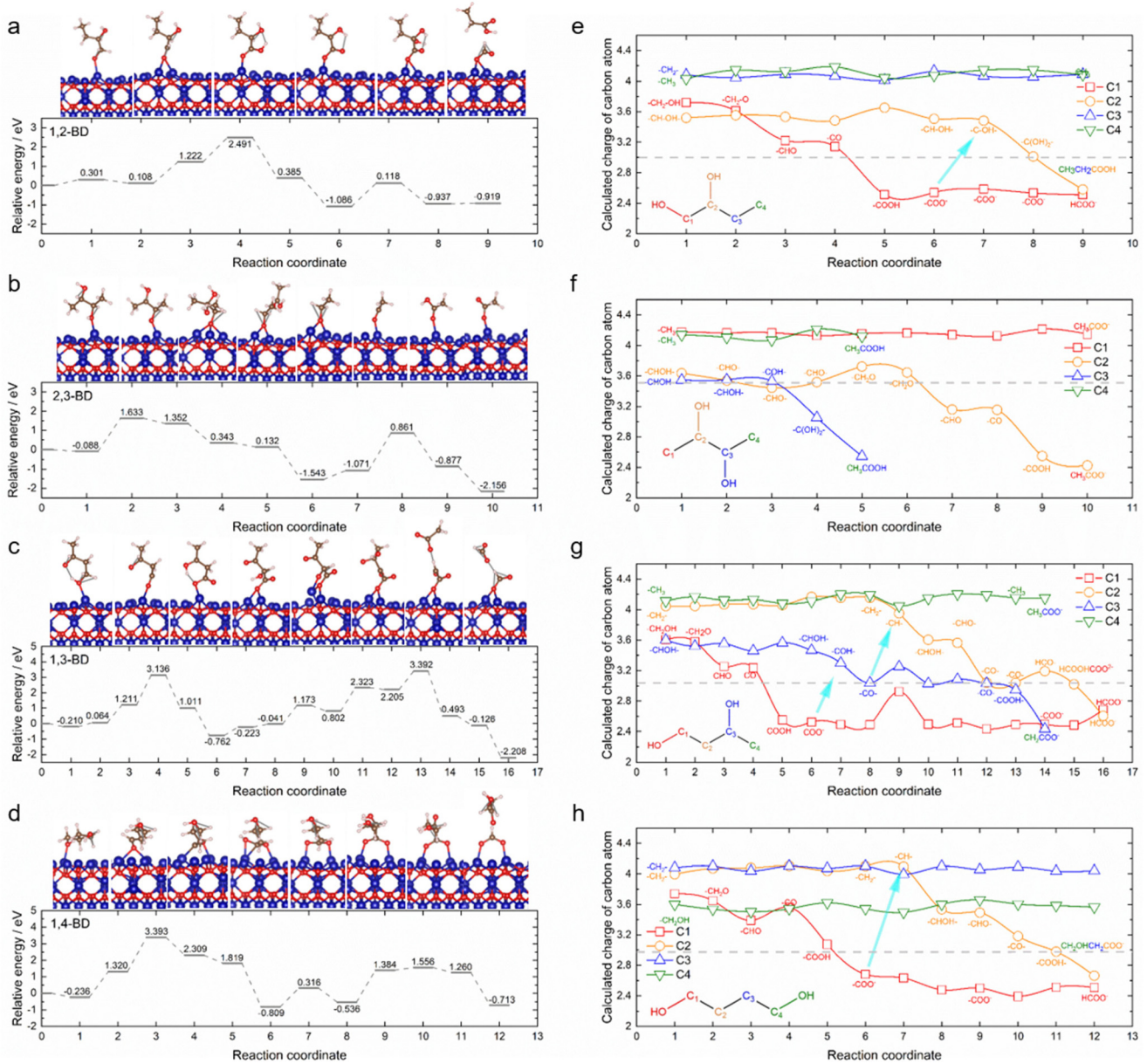

Fig. 3 The representative diagram, system energy (left), and the carbon charge (right) of butanediol oxidation on the Co_3O_4-(111) surface for (a) and (e) 1,2-butanediol (1,2-BD), (b) and (f) 2,3-butanediol (2,3-BD), (c) and (g) 1,3-butanediol (1,3-BD), and (d) and (h) 1,4-butanediol (1,4-BD).

oxidation do not happen on the C2 atom but happens on the C3 atom with a hydroxyl group, where –CHOH– becomes –COH– and further –CO–. In comparison with –CO– at the C1 atom, the –CO– at C2 does not become a carboxylic group. Instead, $–CH_2–$ at the C2 atom follows –CH–, –CHOH–, and –CHO– to form –CO–. Next, –CO– at the C3 atom continues to be oxidized to –COOH. At this time, C2–C3 bond cleavage happens. Moreover, the C3–C4 species become CH_3COO^- to dissolve in the solution. The adsorbed C1–C2 species further become $HCOOHCOO^{2-}$ followed by C1–C2 bond cleavage to form HCOO–. From the energy aspect, the highest energy change before the C–C bond cleavage occurs during the carbonyl or carboxylic group formation. For 1,4-BD oxidation (Fig. 3d and h), firstly the adsorbed C1 group dehydrogenates and is oxidized to the carboxylic group, which is consistent with 1,2-BD and 1,3-BD oxidation. Then there are two different reaction pathways for C4 terminal group and C2 group oxidation. In C4 terminal group oxidation, $–CH_2OH$ also becomes a carboxylic group by dehydration and oxidation, and forms succinate without C–C bond cleavage. The other reaction pathway takes place at the C2 group and it changes from $–CH_2–$ to a carboxylic group, and then C1–C2 bond cleavage happens and forms formate and 3-hydroxypropionate. Moreover, 1,4-BD has another oxidation pathway, where no C–C bond cleavage occurs, and the hydroxyl groups are oxidized to carboxylic groups instead (Fig. S8†). 2,3-BD as a secondary

alcohol has a different reaction step from the primary alcohol (Fig. 3b and f). First, the adsorbed C2 group –CHOH– becomes –CHO– by dehydrogenation on the hydroxyl group. Then the C3 group –CHOH– becomes –COH– by dehydrogenation of the C–H group, and further forms $–C(OH)_2–$. Next, the C2–C3 bond cleavage happens, and the terminal part becomes acetate. The remaining C1–C2 part becomes acetate by dehydrogenation and oxidation. The carbon charges of 1,3-BD, 1,4-BD, and 2,3-BD show a similar trend to that of 1,2-BD during the dehydrogenation and oxidation process.

The highest energy changes before the C–C bonding cleavage are 2.491, 1.633, 3.136, and 3.393 eV for 1,2-BD, 2,3-BD, 1,3-BD, and 1,4-BD, respectively. Except for 2,3-BD, the calculation results indicate that the butanediol reactivities follow the order of 1,2-BD > 1,3-BD > 1,4-BD, which is consistent with the experimental results. A closer position of hydroxyl groups is therefore considered capable of lowering the energy gap of the butanediol oxidation reaction and eventually promoting the butanediol electro-oxidation reactivity. This explains the experimental observation that vicinal hydroxyl groups promote the C–C bond cleavage during the electro-oxidation as it reduces the energy gap. 2,3-BD has the lowest energy gap, probably because it experiences a different oxidation pathway without a carbonyl group compared to primary butanediols. This result is consistent with the experimental observation that the vicinal hydroxyl groups promote butanediol oxidation.

Fig. 4 focuses on the charge change of the carbon atoms participating in the C–C bond cleavage. It is noted that the carbon charge in the C–C bond to be cleaved is higher than 3.5. In the step before the C–C bond cleavage, the carbon charges become low. For vicinal butanediols 1,2-BD and 2,3-BD, the carbons with hydroxyl groups comprise the C–C bond to be cleaved. The initial charge of the carbon atoms with the hydroxyl group (the C1 atom in 1,2-BD and the C2 atom in 2,3-BD) as the adsorption site is slightly higher than that of the other carbon atoms. In 1,2-BD, the charge of the C1 atom decreases by 1.19 to 2.53, while the decrease of charge density at the C2 atom is merely 0.51. It shows that the charge change at the carbon atoms to be cleaved is very different. A dramatic change happens on the carbon atoms, in which the hydroxyl group is adsorbed on Co. In comparison with 1,2-BD, 2,3-BD has less charge change at the carbon atoms. The charge change at the C2 atom is as low as 0.12. In the step before C–C bond cleavage, the charge is still 3.52. The charge of the C3 atom decreases from 3.55 to 3.05. In 1,3-BD, as a non-vicinal butanediol, the carbon atoms C2 and C3 are not closest to the adsorption site, the charge of the C2 atom without the hydroxyl group is obviously higher than that of the C3 atom with the hydroxyl group, and the C2 atom experiences a more dramatic change than the C3 atom. For 1,4-BD, the charge of the C2 atom without the hydroxyl group is higher than that of the C1 atom with its hydroxyl group adsorbed on Co. The C1 atom has a higher charge decrease than the C2 atom. It is noted that for 1,2-BD, 1,3-BD, and 1,4-BD, the carbon charge decreases to below 3.1 before the C–C bond cleavage step. This suggests that the carbon atom becomes more active when having a low charge. An exception is 2,3-BD, where one carbon atom charge is below 3.1, and the other one is almost 3.5. This means a lesser charge change is needed for its C–C bond cleavage.

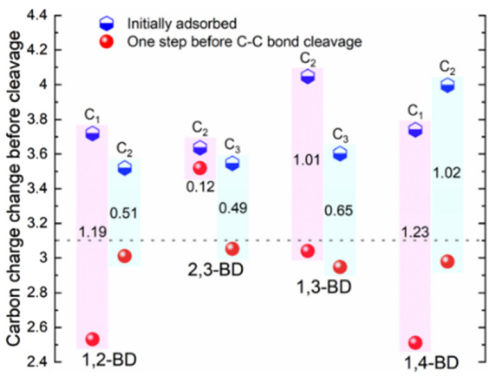

Fig. 4 The charge of carbon in the C–C bond to be cleaved, from the initial state to the state prior to cleavage. The magenta columns represent the carbon closest to the adsorption sites and the cyan columns represent the other carbon in the C–C bond to be cleaved.

3. Conclusions

In summary, a systematic investigation has been conducted on the hydroxyl group position effect in the electro-oxidation of butanediols on Co_3O_4 in alkaline media. It is concluded that the electro-oxidation reactivities of these butanediols are in the order of 1,2-BD > 2,3-BD > 1,3-BD > 1,4-BD. Vicinal butanediols are more reactive, and the closer the two hydroxyl groups are, the more easily the alcohols are oxidized. This indicates that the position of hydroxyl groups plays an important role in determining the reactivity of butanediols. Besides, the HPLC and NMR analyses of butanediol oxidation products show that vicinal hydroxyl groups promote C–C bond cleavage in addition to increased reactivity. Moreover, the product analysis also shows that some valuable compounds, such as 3-hydroxypropionic acid (3-hydroxypropionate) can be synthesized by the C–C bond cleavage and selective oxidation of 1,4-BD. The calculations show that the charge density of carbon atoms in the C–C bond to be cleaved decreased dramatically before cleavage. These results provide accessible routes for the preparation of value-added products with high selectivity from the electrochemical oxidation of butanediols. In addition, due to the much lower potential of diol oxidation than that of the OER, the diol oxidation reaction may be a promising alternative anode reaction to be studied in the future for co-generation of hydrogen and high-value chemicals.

Conflicts of interest

There are no conflicts to declare.

Acknowledgements

This work was supported by the Singapore Ministry of Education Tier 2 Grants (MOE-T2EP10220-0001), the Singapore National Research Foundation under its Campus for Research Excellence and Technological Enterprise (CREATE) programme and NRF Fellowship (NRF-NRFF2017-04), the Centre of Advanced Catalysis Science and Technology, Nanyang Technological University, and the Agency for Science, Technology and Research (Central Research Fund Award). The authors thank the Facility for Analysis, Characterisation, Testing and Simulation (FACTS) in Nanyang Technological University for materials characterization.

References

1 S. Möhle, M. Zirbes, E. Rodrigo, T. Gieshoff, A. Wiebe and S. R. Waldvogel, *Angew. Chem., Int. Ed.*, 2018, **57**, 6018–6041.
2 C. Dai, L. Sun, H. Liao, B. Khezri, R. D. Webster, A. C. Fisher and Z. J. Xu, *J. Catal.*, 2017, **356**, 14–21.
3 D. Wang, P. Wang, S. Wang, Y.-H. Chen, H. Zhang and A. Lei, *Nat. Commun.*, 2019, **10**, 2796.
4 Z. Li, Y. Yan, S.-M. Xu, H. Zhou, M. Xu, L. Ma, M. Shao, X. Kong, B. Wang, L. Zheng and H. Duan, *Nat. Commun.*, 2022, **13**, 147.
5 C. Tang, Y. Zheng, M. Jaroniec and S.-Z. Qiao, *Angew. Chem., Int. Ed.*, 2021, **60**, 19572–19590.
6 Y. Kwon, K. J. P. Schouten and M. T. M. Koper, *ChemCatChem*, 2011, **3**, 1176–1185.
7 Y. Kwon, S. C. S. Lai, P. Rodriguez and M. T. M. Koper, *J. Am. Chem. Soc.*, 2011, **133**, 6914–6917.
8 J. Li, S. Z. Jilani, H. Lin, X. Liu, K. Wei, Y. Jia, P. Zhang, M. Chi, Y.-Y. J. Tong, Z. Xi and S. Sun, *Angew. Chem., Int. Ed.*, 2019, **58**, 11527–11533.
9 L. Fan, Y. Ji, G. Wang, J. Chen, K. Chen, X. Liu and Z. Wen, *J. Am. Chem. Soc.*, 2022, **144**, 7224–7235.
10 Y. Li, X. Wei, S. Han, L. Chen and J. Shi, *Angew. Chem., Int. Ed.*, 2021, **60**, 21464–21472.
11 N. Logeshwaran, I. R. Panneerselvam, S. Ramakrishnan, R. S. Kumar, A. R. Kim, Y. Wang and D. J. Yoo, *Adv. Sci.*, 2022, **9**, 2105344.
12 B. Zhou, Y. Li, Y. Zou, W. Chen, W. Zhou, M. Song, Y. Wu, Y. Lu, J. Liu, Y. Wang and S. Wang, *Angew. Chem., Int. Ed.*, 2021, **60**, 22908–22914.
13 R. Ge, Y. Wang, Z. Li, M. Xu, S.-M. Xu, H. Zhou, K. Ji, F. Chen, J. Zhou and H. Duan, *Angew. Chem.*, 2022, **61**, e202200211.
14 J. E. Sulaiman, S. Zhu, Z. Xing, Q. Chang and M. Shao, *ACS Catal.*, 2017, **7**, 5134–5141.
15 J. Suntivich, Z. Xu, C. E. Carlton, J. Kim, B. Han, S. W. Lee, N. Bonnet, N. Marzari, L. F. Allard, H. A. Gasteiger, K. Hamad-Schifferli and Y. Shao-Horn, *J. Am. Chem. Soc.*, 2013, **135**, 7985–7991.
16 L. Dai, Q. Qin, X. Zhao, C. Xu, C. Hu, S. Mo, Y. O. Wang, S. Lin, Z. Tang and N. Zheng, *ACS Cent. Sci.*, 2016, **2**, 538–544.
17 S. Sun, L. Sun, S. Xi, Y. Du, M. U. A. Prathap, Z. Wang, Q. Zhang, A. Fisher and Z. J. Xu, *Electrochim. Acta*, 2017, **228**, 183–194.
18 S. Sun and Z. J. Xu, *Electrochim. Acta*, 2015, **165**, 56–66.
19 J. B. Wu, Z. G. Li, X. H. Huang and Y. Lin, *J. Power Sources*, 2013, **224**, 1–5.
20 L. Qian, L. Gu, L. Yang, H. Yuan and D. Xiao, *Nanoscale*, 2013, **5**, 7388–7396.
21 M. Betowska-Brzezinska and T. Uczak, *J. Appl. Electrochem.*, 1997, **27**, 999–1011.
22 M. Beltowska-Brzezinska, T. Luczak and R. Holze, *Surf. Sci.*, 1998, **418**, 281–294.
23 A. Hilmi, E. M. Belgsir, J. M. Leger and C. Lamy, *J. Electroanal. Chem.*, 1995, **380**, 177–184.
24 R. Holze, T. Luczak and M. Beltowska-Brzezinska, *Electrochim. Acta*, 1994, **39**, 485–489.
25 T. Luczak, M. Beltowska-Brzezinsk and R. Holze, *Electrochim. Acta*, 1993, **38**, 717–720.
26 R. Holze, T. Luczak and M. Beltowska-Brzezinska, *Electrochim. Acta*, 1990, **35**, 1345–1350.
27 D. Takky, B. Beden, J.-M. Leger and C. Lamy, *J. Electroanal. Chem.*, 1985, **193**, 159–173.
28 A. J. Bard and L. R. Faulkner, *Electrochemical methods: fundamentals and applications*, Wiley-VCH, New York, 2nd edn, 2001.
29 S. S. Bhagwat, Y. Li, Y. R. Cortés-Peña, E. C. Brace, T. A. Martin, H. Zhao and J. S. Guest, *ACS Sustainable Chem. Eng.*, 2021, **9**, 16659–16669.
30 R. Holze and M. Beltowska-Brzezinska, *Electrochim. Acta*, 1985, **30**, 937–939.
31 R. Holze and M. Beltowska-Brzezinska, *J. Electroanal. Chem.*, 1986, **201**, 387–396.
32 B. N. Zope, D. D. Hibbitts, M. Neurock and R. J. Davis, *Science*, 2010, **330**, 74–78.